HHS Public Access

Author manuscript

Dent Mater. Author manuscript; available in PMC 2022 November 16.

Published in final edited form as:

Dent Mater. 2019 September ; 35(9): 1300–1307. doi:10.1016/j.dental.2019.05.025.

Effect of Biomimetic Mineralization on Enamel and Dentin: A Raman and EDX analysis

Arndt Guentsch[1,2], **Mina D. Fahmy**[1], **Constanze Wehrle**[2], **Stefan Kranz**[2], **Sandor Nietzsche**[3], **Jürgen Popp**[4,5], **David C. Watts**[6], **Christoph Krafft**[4], **Bernd W. Sigusch**[2]

[1]Marquette University School of Dentistry, Milwaukee, WI, USA

[2]Clinic of Conservative Dentistry and Periodontology, Center of Dental Medicine, Jena University Hospital, Friedrich-Schiller University Jena, Germany

[3]Center of Electron Microscopy, Friedrich-Schiller University Jena, Germany

[4]Leibniz Institute of Photonic Technology (IPHT), Jena, Germany

[5]Institute of Physical Chemistry and Abbe Center of Photonics, Friedrich-Schiller University Jena, Germany

[6]School of Dentistry and Photon Science Institute, University of Manchester, Manchester, UK

Abstract

Objective.—To investigate the effect of an experimental biomimetic mineralization kit (BIMIN) on the chemical composition and crystallinity of caries-free enamel and dentin samples *in vitro*.

Methods.—Enamel and dentin samples from 20 human teeth (10 for enamel; 10 for dentin) were divided into a control group without treatment and test samples with BIMIN treatment. Quantitative analysis of tissue penetration of fluoride, phosphate, and calcium was performed using energy-dispersive X-ray spectroscopy (EDX). Mineralization depth was measured by Raman spectroscopy probing the symmetric valence vibration near 960 cm^{-1} as a marker for crystallinity. EDX data was statistically analyzed using a paired t-test and Raman data was analyzed using the Student's t-test.

Results.—EDX analysis demonstrated a penetration depth of fluoride of 4.10 ± 3.32 μm in enamel and 4.31 ± 2.67 μm in dentin. Calcium infiltrated into enamel 2.65 ± 0.64 μm and into dentin 5.58 ± 1.63 μm, while the penetration depths for phosphate were 4.83 ± 2.81 μm for enamel and 6.75 ± 3.25 μm for dentin. Further, up to 25 μm of a newly mineralized enamel-like layer was observed on the surface of the samples. Raman concentration curves demonstrated an increased degree of mineralization up to 5 –10 μm into the dentin and enamel samples.

Significance.—Biomimetic mineralization of enamel and dentin samples resulted in an increase of mineralization and a penetration of fluoride into enamel and dentin.

Corresponding author: Dr. Arndt Guentsch, Department of Surgical Sciences, Marquette University School of Dentistry, P.O. Box 1881, Milwaukee, WI 53201-1881, P +1.414.288.6089, F +1.414.288.8329, arndt.guentsch@marquette.edu.

The authors declare to have no conflict of interest.

Keywords

Biomimetic; Mineralization; Enamel; Dentin; Raman; EDX

1. Introduction

Enamel is said to be the hardest tissue of the human body and is also the most mineralized at 96%. The primary mineral present is a crystalline calcium phosphate called hydroxyapatite [1]. It is evident that enamel is not capable of self-repair or regeneration de novo due to the loss of ameloblasts during the maturation process [1]. Dentin is a bone-like matrix consisting of also hydroxyapatite with a mineralization degree of approximately 70% [2]. Unlike enamel, dentin can continuously be formed throughout life time and also in response to external stimuli such as caries formation [3, 4]. This so-called process of tertiary dentin formation is directed towards the dental pulp and can be either reactionary or reparative [5, 6].

However, chemical and physical alterations may lead to a loss of enamel and dentin [7]. Currently, dental materials that can be used for restoration or repair do not show any significant regeneration potential [8]. Thus, investigations are underway to develop new materials which can potentiate regeneration of enamel and dentin tissue [9–12]. Reconstructing enamel-like layers on teeth is consequently an important area of research and biomimetic materials may play a significant role in this process [8, 13, 14]. Regeneration by biomimetic mineralization is a non-invasive technique and does not rely on the function of cells [15]. The natural process of biomineralization is mimicked by developing inorganic-organic hybrid materials which simulates natural mineralized tissues. A variety of biomimetic mineralization methods have been reported already. These methods rely on agarose hydrogel containing calcium chloride [16], nano-complexes of phosphorylated chitosan and amorphous calcium phosphate [17], hydrogen peroxide containing calcium and phosphate paste [18], controlled release of calcium from Ca-EDTA [19], surfactant assembly hydroxyapatite [20], self-assembly of amphiphilic dendrons [21], electrolytical deposition at 85°C [22], amelogenin [23], gelatin-templated mesoporous silica biomaterial [24], and self-assembled oligopeptide amphiphile [25].

In a recent study, our group reported on the successful clinical application of an experimental biomimetic mineralization-kit (BIMIN) in treating dentin hypersensitivity in patients with exposed dentinal tubules by establishing a mineralized enamel-like layer [26]. This principle was also shown to succeed on enamel surfaces *in vivo* [27]. Further, it was evident by X-ray diffraction analysis of a powder sample that the new mineralized layer contained fluorapatite, which is more resistant to decay than normal hydroxyapatite.

The purpose of this study was to investigate whether biomimetic mineralization using BIMIN is merely a result of sedimentation or if there is also penetration of components in the treated enamel and dentin samples. The latter is important for long-term stability and therapeutic effects, e.g. treatment of enamel and dentin lesions as well as treatment of dentin hypersensitivity in clinical practice. We further hypothesized that the application of

the biomimetic mineralization-kit will increase crystallinity as well as the mineral content of the treated samples.

2. Materials and Methods

2.1 Sample preparation

Enamel samples were attained from human caries-free upper central incisors extracted due to hopeless periodontal prognosis and dentin samples from non-erupted third molars (each n = 10). Central incisors were chosen since they provided the largest plane enamel surface, while molars allowed to obtain big dentin samples. The use of human tissue was approved by the ethics committee of the university hospital Jena, Germany (#83154-06/11).

Teeth were prepared as described previously by Beyer *et al.* [28]. In brief, the roots were carefully removed after extraction. In molars, sections were cut from the tooth crowns with a low-speed saw (Isomet, Buehler GmbH, Duesseldorf, Germany) using a water-cooled diamond blade (Buehler GmbH, Duesseldorf Germany) until dentin was fully exposed. For more convenient handling and for stabilization reasons, molar dentin samples and the crowns of the incisors were embedded in a resin (Stycast 1266, Emerson & Cuming ICI, Westerlo, Belgium). In the incisor samples, the resin was cut back until enamel was completely exposed. The samples were then ground with SiC paper (grit 1200 to 4000; Buehler GmbH, Duesseldorf, Germany). Afterwards, the samples were cleaned in an ultrasonic bath of distilled water (Transsonic T310, Bender & Hobein GmbH, Bruchsal).

2.2 Biomimetic mineralization treatment

One half of the surface of each sample was covered with PVC tape (Tesa AG, Hamburg, Germany) to obtain an untreated (UT) control area, the other half was treated with the biomimetic mineralization-kit (BIMIN). The BIMIN-application followed a previously described protocol [27]. First, the test sides of the samples were treated with 24% EDTA solution which was applied to the surface for 2 minutes (Pref Gel, Straumann, Freiburg, Germany) to remove any existing smear layers. The experimental biomimetic mineralization system (Heraeus Kulzer GmbH, Hanau, Germany) itself was composed of an alkaline pretreatment solution containing calcium ions (pH = 9), a gelatin gel containing phosphate and fluoride ions, and a gelatin gel containing calcium ions. The pretreatment solution was used to increase the attractiveness of the tooth surface to mineralization and allowed guided mineralization towards the tooth surface. After moistening the tooth surface with the pretreatment solution, the gel-films were placed onto the tooth surface via a sandwich technique, where the phosphate-gel was in contact with the sample and covered by the calcium-gel. The samples were then stored in an incubator (BED 53, WTB BINDER Labortechnik GmbH, Tuttlingen, Germany) at 37 °C to simulate oral cavity conditions. The BIMIN gels were gently removed after 12 hours under flowing water and the surface was cleaned using an extra-soft toothbrush. Pilot tests demonstrated that a single treatment resulted in inhomogeneous surfaces. Therefore, the application of the biomimetic mineralization kit was repeated four more times (in total 5 treatments) to assure reliable measurements. For further analysis the samples were cross-sectioned in the middle of the sample in right-angle to the treated/untreated areas.

2.3 SEM/EDX analysis

In preparation for SEM/EDX, the treated samples were dried for ten days in a desiccator. The samples were then mounted on stubs using the conductive glue “Leit-C” (Plano GmbH, Wetzlar, Germany). The samples were vacuum coated with approximately 14 nm thickness of carbon to reduce electrostatic charging with a BAL-TEC SCD 005 Sputter Coater (BAL-TEC AG, Liechtenstein). All of the treated samples prepared for SEM were examined using a SEM LEO-1450 (Carl Zeiss AG, Oberkochen, Germany) equipped with a QUANTAX 200 detector (Bruker GmbH, Berlin, Germany) at 12 kV for EDX analysis. The EDX measurement used a spot size of 50 nm. The spatial resolution of the EDX technique is determined by the size of the interaction volume of the beam electrons and the sample material and was estimated to be approx. 1.6 μm for the given experimental set-up using the CASINO modeling tool [29]. The penetration of minerals in the enamel and dentin samples were analyzed at three different measuring lines of 30 μm length, each in parallel distance of 2 μm. The measurements were performed on the surface of the cross-sections, starting at the outer layer (treated/untreated surface) moving pulp-wards. In total, 50 measurements were taken every 0.6 μm per line. The representative measurement areas were selected under 2000x magnification. No dentinal tubules were crossed in the dentin samples. The content of fluoride, phosphate, and calcium (as main compartments of the biomimetic mineralization kit) were analyzed at each measurement point.

In order to evaluate the penetration depth of the BIMIN main components (Ca, P, F) into the hard tissue the measured concentration gradient was curve-fitted by a simplified diffusion profile *c(x)* for each element as a solution of the one-dimensional, stationary diffusion equation following Fick’s law:

$$c(x) = c_{10} + (c_0 - c_{10}) \cdot e^{-\left(\frac{x - x_0}{x_p}\right)^2} \; for \; x > 0$$

The concentration of the elements in the BIMIN layer was said to be c_0 and the bulk concentration in the hard tissue was taken at 10 μm depth as c_{10}. The BIMIN / hard tissue junction was said to be x_0. The use of this fit allows quantifying a penetration depth which was said to be x_p where the concentration was dropped to 1/e of the initial value.

2.4 Collection and analysis of Raman data

A single mode diode laser (model Xtra, Toptica, Germany) at 785 nm emission was coupled via a single mode fiber to a Raman microscope for excitation. The microscope was coupled via a multi-mode fiber to the Raman spectrometer (RXN1 microprobe, Kaiser Optical System, USA). The laser light with an intensity of 100 mW was focused on the sample using a 60×/NA 1.0 water immersion objective (Nikon, Japan). During data acquisition the sample was immersed in water. The advantage of the water immersion objective lens was its high numerical aperture of 1.0 giving high lateral resolution due to high microscopic confocality and effective signal collection. Furthermore, drying effects were avoided. The Raman signal was detected on a Peltier-cooled (−60°C), back-illuminated, deep-depletion CCD chip (Andor, Ireland). Lines of 50 Raman spectra were obtained over the spectral region of 200 to 3450 cm^{-1} at a spectral resolution of 4 cm^{-1} with a step size of 1 μm

and 1 second exposure time per spectrum. The Holograms software (Kaiser) automatically performed corrections of dark counts, cosmic spikes, and calibrations of the wavenumber and intensity axis. The Holomap software (Kaiser) that runs under Matlab (The Mathworks, USA) was used for data analysis. The MCR (multivariate curve resolution) algorithm decomposed the data sets into weights and vectors that represent the concentrations and spectral contributions, respectively, of hydroxyapatite, BIMIN, embedding material and background. The MCR analysis was performed on the combined data sets of control and test samples in the spectral range from 900 to 1020 cm^{-1}. Extending the range did not improve the results. Furthermore, the full width at half maximum (FWHM) of the hydroxyapatite band near 960 cm^{-1} was calculated to determine the crystallinity of dentin, enamel and BIMIN [30].

2.5 Statistical analysis

The statistical analysis was conducted using SPSS 22 (IBM SPSS Statistics, New York, USA). The mean and standard deviation for the concentrations of fluoride, phosphate, and calcium were calculated for the newly mineralized layer, the penetration zone (interface of BIMIN-layer and tooth sample) and the bulk zone (c_{10}) of the samples. The penetration of the elements was analyzed using a paired t-test. The level of significance was set at $p < 0.05$.

3. Results

3.1 SEM/EDX

The mineral composition of treated (at BIMIN/hard tissue junction x_0) and untreated (at surface) samples are listed in table 1. For all measured elements, higher mass concentrations were detected in the treated tooth samples. The detected difference in fluoride concentration between treated and untreated samples for enamel was 2.2 ± 0.9 % vs. 1.6 ± 1.0 % (not significant) and for dentin 6.2 ± 2.1 % vs. 3.1 ± 1.2 % ($p < 0.05$). Further, EDX analysis showed that fluoride penetrated 4.1 ± 3.3 μm in enamel and 4.3 ± 2.7 μm in dentin. On all treated samples an enamel-like layer was detectable (Fig. 1). Figure 2 demonstrates an EDX output of representative enamel and dentin samples. The penetration depth (x_p) of calcium into enamel was 2.7 ± 0.6 μm and into dentin 5.6 ± 1.6 μm. An increase in phosphate was detected up to 4.8 ± 2.8 μm in enamel and 6.8 ± 3.3 μm in dentin samples.

3.2 Raman data

Figure 3 shows Raman spectra of dentin, enamel and BIMIN. The spectra were normalized relative to the most intense band near 960 cm^{-1} which was assigned to the symmetric stretch vibration of PO_4^{3-} in hydroxyapatite [30]. This band was centered at 960 cm^{-1} in enamel and dentin, and at 963 cm^{-1} in BIMIN. Another prominent spectral feature was the FWHM of the hydroxyapatite band. FWHM was 12.5 cm^{-1} for enamel, 12.2 cm^{-1} for BIMIN and 16.6 cm^{-1} for dentin. Further bands in dentin at 1248, 1452 and 1666 cm^{-1} were assigned to the organic matrix, mainly collagen. The band at 1637 cm^{-1} was assigned to water and the intensity of this band relative to the band at 960 cm^{-1} was reduced in enamel and BIMIN. Bands at 430, 587, 1005 and 1044 cm^{-1} were assigned to other modes of hydroxyapatite while the band at 1070 cm^{-1} was due to carbonate. In summary, applying spectral features

between 900 and 1020 cm^{-1} allowed the distinguishing of the components and monitoring of the transition and thickness of the BIMIN layer.

The upper portion of figure 4 shows representative photomicrographs of dentin and enamel with and without a fivefold BIMIN treatment, respectively. The blue plus signs indicate the start and end points of the Raman line which are 50 μm apart. The circumpulpal dentin and dentin tubules, as well as the BIMIN layer were clearly visible in dentin samples. Enamel structures and the BIMIN layer were vaguely distinguishable in enamel samples. The MCR intensity of the hydroxyapatite component increased from the starting point to a maximum near 20 μm for both control samples. Between 20 and 50 μm the hydroxyapatite component slightly decreased for all samples. The BIMIN component was negligible in control samples, as expected. Below 10 μm the FWHMs of the hydroxyapatite band were inconclusive because the intensities near the margins were very weak. The FWHM was near 16 for dentin and near 12.5 for enamel which was consistent with the higher crystallinity of enamel. The transition from BIMIN to dentin and enamel showed characteristic features. From the BIMIN component and the crystallinity index, the width of the BIMIN layer can be determined near 25 μm in dentin with two well-resolved maxima corresponding to the newly mineralized layer at the surface and the penetration zone, respectively, and 10 μm in enamel with just one maximum located at the surface. The deeper penetration of BIMIN seems to be a consequence of the dentinal tubules present in dentin. The FWHM as crystallinity index, decreased from 16 towards 12.2 in dentin and from 12.5 towards 12.4 in enamel.

BIMIN treatment resulted in precipitation of layers with mean values of 24.5 ± 5.1 μm on dentin and 13.2 ± 3.3 μm on enamel. Therefore, the layers on dentin samples were significantly thicker compared to the enamel samples ($p < 0.05$). Careful inspection of the BIMIN layers revealed an inhomogeneous layer of thicknesses (not shown) that requires further optimization of the treatment process and more detailed Raman studies with extended regions of interest.

4. Discussion

This *in vitro* study demonstrated that the application of an experimental biomimetic mineralization kit increased the crystallinity and mineral content in enamel and dentin samples due to a penetration of fluoride, calcium, and phosphate. A newly formed mineral layer was detected on all treated samples with heights ranging in between 13 and 25 μm for enamel and dentin, respectively.

Previous studies have suggested that a low mineral content of enamel leads to a higher susceptibility for dental caries [31, 32]. Further, the degree of porosity and the chemical composition in general determine the degree of solubility of dental hard tissues in contact to acidic solutions [33]. A recent study analyzed the mineral content of human enamel and found that mineralization varies between individuals, but moreover cervical enamel showed less mineralization compared to other regions [34]. It was concluded that less mineralized areas might be susceptible to the formation of caries in a stronger way. A layer of fluoroapatite, which is less soluble compared to hydroxyapatite applied on the enamel

surface should offer considerable protection for caries [35]. In an earlier study our group confirmed by X-ray diffraction of a powder sample that the newly formed mineral layer after applying of BIMIN mainly consists of fluoroapatite [27].

In the past, Hannig and Hannig reviewed several studies that examined the biomimetic synthesis of enamel [36]. They concluded that crystal formation only occurred under purely *in vitro* conditions, thus overlooking the physiology of the human oral cavity. However, our group used the biomimetic mineralization kit to successfully treat dentinal sensitivity by establishing a mineralized layer which sealed the eroded dentinal tubules. This previous published work clearly showed that a biomimetic layer of enamel can be formed also *in vivo* which further remained stable for at least one year [26]. The biomimetic mineralization-kit BIMIN was applied *in vitro* in the present study, but the oral environment was simulated in terms of temperature and moisture.

Cao and colleagues found that the enamel matrix derivative (EMD) promoted *in vitro* biomimetic mineralization as well as enamel prism-like formation onto demineralized tooth samples [37]. They also demonstrated that enamel prism-like tissue can be regenerated in an agarose hydrogel biomimetic mineralization model [16]. Similarly Ning *et al.* concluded that etched dentin after being treated with the biomimetic mineralization system of agarose gel loaded with calcium phosphate showed a significant formation of crystals on the dentinal surface after five applications [38]. However, it was identified that further work was needed to be carried out to determine the stability of the EMD- agarose hydrogel model in the oral cavity. Kwak *et al.* recently demonstrated that the combination of inorganic pyrophosphate and leucine-rich amelogenin peptide allows to regulate the shape and orientation of growing enamel crystals [14]. After an application on acid-etched enamel samples over 20 hours they observed a densely packed mineral layer of hydroxyapatite crystals.

As noted earlier, the main purpose of restorative materials currently available, such as composites, is to merely replace lost tooth hard tissue while they evidently are also capable of improving function and aesthetics. These materials however have only very few structural similarities to natural tooth structure and more importantly do not allow any potential tissue regeneration [36]. In recent years, several attempts have been made to create synthetic dental enamel and to support repair [38]. Lippert and colleagues showed that a hydroxyapatite layer can be deposited from a solution onto enamel *in vitro* [39]. Moreover, other studies have shown that an artificially crystalline fluoroapatite of similar structure to human enamel may be created [18]. The limitations of such studies however, can be seen in the experimental conditions (temperatures between 200°C and 600° C) that are far away from those observed in the human oral cavity. The synthesis of fluoroapatite nanorods of varying sizes, shapes, and composition for incorporation into dental materials or in the treatment and prevention of caries has also been reported [39]. Despite these advancements, many of the artificially created hydroxyapatites have not been completely effective in enamel repair and remineralization [40]. The results of this study showed, that a newly formed BIMIN-layer of 13.2 ± 3.2 μm was detectable on the outer surface of enamel samples. Additionally, it was shown that e.g., fluoride penetrated 4.1 ± 3.3 μm into enamel.

Biomimetic remineralization of dentin has been investigated with different methods using ion-containing solutions or ion leaching silicon-containing materials. Gandolfi *et al.* discussed the use of bioactive “smart” composite materials containing reactive calcium-silicate Portland-derived mineral powder as tailored fillers and showed that apatite-depleted dentin surfaces could be remineralized using a dentin-disc model [41]. The biomimetic formation of apatite may depend on the presence of gelatin based scaffolds [42] such as those used in our experimental methods. Ning *et al.* recently introduced an experimental method for biomimetic mineralization of hydroxyapatite [38]. They used agarose gel containing Na2HPO4 that covered an acid-etched dentin slice. Comparable to a sandwich-technique, this gel was then covered by a layer of agarose gel without phosphate ions, masked by a $CaCl_2$ solution. This system was then kept in a water bath at 37° C. After 10 days of biomimetic mineralization in vitro, Ning and colleagues observed densely packed hydroxyapatite crystals that covered the dentin surface and occluded the dentinal tubules. The use of fluoride-enriched phosphate gelatin-gel and calcium loaded gelatin-gel in this study resulted in the newly formation of a mineral layer at the surface of the dentin samples with a width of approximal 24.5 ± 5.1 μm. Moreover, fluoride penetrated 4.3 ± 2.7 μm into the dentin samples and Raman analysis revealed that the crystallization of both, enamel and dentin increased after BIMIN treatment.

Dentin is a complex tissue that basically contains apatite, collagens and other proteins as well as water. Methods of remineralization of dentin include the simple precipitation of mineral into the loose demineralized dentin matrix between collagen fibrils (net remineralization) or the chemical tight association of mineral to the dentin matrix structure (functional remineralization) [43, 44]. Busch *et al.* suggested that because the sequence of amino acids in collagen and acid-hydrolyzed gelatin is essentially identical, polar regions that share similarities are expected to act as nucleation centers in gelatin (Busch et al. 2004). The peptides originating from gelatin of the experimental mineralization-kit used may orientate perpendicular to the substrate and parallel to each other. Polar regions on the molecules attract ions that mineralize apatite, templated by the ordered gelatin. This leads to the perpendicular growth of fluorapatite crystals. The long axis of apatite and gelatin fibers are preferentially oriented parallel to each other.

In this study, we hypothesized that the introduced experimental biomaterial may lead to (at least superficial) functional remineralization in existing dentin structures in addition to mineralization of an enamel-like fluorapatite layer.

In conclusion, the treatment of enamel and dentin samples resulted in the mineralization of an enamel-like fluoroaptite layer, which evidently seems to be bonded to the underlying tooth structure. Raman spectroscopy demonstrated an increase in crystallinity and SEM/EDX analysis suggested a penetration of calcium, phosphate, and fluoride into the treated enamel and dentin samples. In future studies the effect on demineralized samples should also be observed.

Acknowledgement

This study was institutional funded using an independent research grant awarded to Dr. Arndt Guentsch. The authors are grateful to Dr. Ulrike Kraft (Friedrich-Schiller-University Jena, Germany) for her help in preparing the samples.

This publication was supported by the National Institutes for Research Resources and the National Center for Advancing Translational Sciences, National Institutes of Health, through Grant Number UL1TR001436. Its contents are solely the responsibility of the authors and do not necessarily represent the official views of the NIH.

5. References

[1]. Bartlett DW, Lussi A, West NX, Bouchard P, Sanz M, Bourgeois D. Prevalence of tooth wear on buccal and lingual surfaces and possible risk factors in young European adults. J Dent. 2013;41:1007–13. [PubMed: 24004965]

[2]. Bertassoni L Denin on the nanoscale: Hierarchical organization, mechanical behavior and bioinspired engineering. Dent Mater. 2017.

[3]. Staines M, Robinson W, Hood J. Spherical indentation of tooth enamel. Journal of materials science. 1981;16:2551–6.

[4]. Nanci A Ten cate's oral histology-pageburst on vitalsource: development, structure, and function: Elsevier Health Sciences; 2007.

[5]. Huang GT-J. Dental pulp and dentin tissue engineering and regeneration– advancement and challenge. Frontiers in bioscience (Elite edition). 2011;3:788. [PubMed: 21196351]

[6]. Smith AJ, Sloan AJ, Matthews JB, Murray PE, Lumley P. Reparative processes in dentine and pulp. Tooth wear and sensitivity Addy M, Embery G, Edgar WM, Orchardson R, editors London: Martin Dunitz. 2000:53–66.

[7]. Kinney JH, Nalla RK, Pople JA, Breunig TM, Ritchie RO. Age-related transparent root dentin: mineral concentration, crystallite size, and mechanical properties. Biomaterials. 2005;26:3363–76. [PubMed: 15603832]

[8]. Jandt KD, Sigusch BW. Future perspectives of resin-based dental materials. Dental materials. 2009;25:1001–6. [PubMed: 19332352]

[9]. Fan Y, Sun Z, Moradian-Oldak J. Controlled remineralization of enamel in the presence of amelogenin and fluoride. Biomaterials. 2009;30:478–83. [PubMed: 18996587]

[10]. Jandt KD. Evolutions, revolutions and trends in biomaterials science–a perspective. Advanced Engineering Materials. 2007;9:1035–50.

[11]. Li X, De Munck J, Yoshihara K, Pedano M, Van Landuyt K, Chen Z, et al. Re-mineralizing dentin using an experimental tricalcium silicate cement with biomimetic analogs. Dental Materials. 2017;33:505–13. [PubMed: 28274489]

[12]. Niu L, Zhang W, Pashley D, Breschi L, Mao J, Chen J, et al. Biomimetic remineralization of dentin. Dent Mater. 2014;30:77–96. [PubMed: 23927881]

[13]. Willems G, Lambrechts P, Braem M, Celis J-P, Vanherle G. A classification of dental composites according to their morphological and mechanical characteristics. Dental Materials. 1992;8:310–9. [PubMed: 1303373]

[14]. Kwak S, Litman A, Margolis H, Yamakoshi Y, Simmer J. Biomimetic enamel regeneration mediated by leucine-rich amelogenin peptide. J Dent Res. 2017;96:524–30. [PubMed: 28113034]

[15]. Cochrane N, Cai F, Huq N, Burrow M, Reynolds E. New approaches to enhanced remineralization of tooth enamel. J Dent Res. 2010;89:1187–97. [PubMed: 20739698]

[16]. Cao Y, Mei ML, Li Q-L, Lo ECM, Chu CH. Agarose hydrogel biomimetic mineralization model for the regeneration of enamel prismlike tissue. ACS applied materials & interfaces. 2013;6:410–20. [PubMed: 24354267]

[17]. Zhang X, Li Y, Sun X, Kishen A, Deng X, Yang X, et al. Biomimetic mineralization of demineralized enamel with nano-complexes of phosphorylated chitosan and amorphous calcium phosphate. J Mater Sci: Mater Med. 2014;25:2619–28. [PubMed: 25074834]

[18]. Yamagishi K, Onuma K, Suzuki T, Okada F, Tagami J, Otsuki M, et al. Materials chemistry: A synthetic enamel for rapid tooth repair. Nature. 2005;433:819. [PubMed: 15729330]

[19]. Chen H, Tang Z, Liu S, Sun K, Chang S, Peters M, et al. Acellular synthesis of a human enamel-like microstructure. Adv Mat. 2006;18:1846–51.

[20]. Fowler C, Li M, Mann S, Mangolis H. Influence of surfactant assembly on the formation of calcium phosphate materials - A model for dental enamel formation. J Mater Chem. 2005;15:3317–25.

[21]. Yang S, He H, Wang L, Jia X, Feng H. Oriented crystallization of hydroxyapatite by the biomimetic amelogenin nanospheres from self-assemblies of amphilic dendrons. Chem Comm. 2011;47:10100–2. [PubMed: 21833384]

[22]. Ye W, Wang X. Ribbon-like and rod-like hydroxyapatite crystals deposited on titanium surface with electrochemical method. Mater Lett. 2007;61:4062–5.

[23]. Fan Y, Sun Z, Wang R, Abbott C, Moradian-Oldak J. Enamel inspired nanocomposite fabrication through amelogenin supramolecular assembly. Biomaterials. 2007;28:3034–42. [PubMed: 17382381]

[24]. Chiang Y, Lin H, Chang H, Cheng Y, Tang H, Yen W, et al. A mesoporous silica biomaterial for dental biomimetic mineralization. ACS Nano. 2014;8:12502–13. [PubMed: 25482513]

[25]. Li Q, Ning T, Cao Y, Zhang W, Mei M, Chu C. A novel self-assembled oligopeptide amphiphile for biomimetic mineralization of enamel. BMC Biotechnology. 2014;14:32. [PubMed: 24766767]

[26]. Guentsch A, Seidler K, Nietzsche S, Hefti AF, Preshaw PM, Watts DC, et al. Biomimetic mineralization: Long-term observations in patients with dentin sensitivity. Dental Materials. 2012;28:457–64. [PubMed: 22305715]

[27]. Guentsch A, Busch S, Seidler K, Kraft U, Nietzsche S, Preshaw PM, et al. Biomimetic mineralization: effects on human enamel in vivo. Advanced Engineering Materials. 2010;12:B571–B6.

[28]. Beyer M, Reichert J, Sigusch BW, Watts DC, Jandt KD. Morphology and structure of polymer layers protecting dental enamel against erosion. Dent Mater. 2012;28:1089–97. [PubMed: 22883479]

[29]. Drouin D, Couture AR, Joly D, Tastet X, Aimez V, Gauvin R. CASINO V2.42—A Fast and Easy-to-use Modeling Tool for Scanning Electron Microscopy and Microanalysis Users. . Scanning. 2007;29:92–101. [PubMed: 17455283]

[30]. Carden A, Morris M. Application of vibrational spectroscopy to the study of mineralized tissues. J Biomed Opt. 2000;5:259–68. [PubMed: 10958610]

[31]. Shellis R Relationship between human enamel structure and the formation of caries-like lesions in vitro. Archives of Oral Biology. 1984;29:975–81. [PubMed: 6598367]

[32]. Targino A, Rosenblatt A, Oliveira A, Chaves A, Santos V. The relationship of enamel defects and caries: a cohort study. Oral Diseases. 2011;17.

[33]. Arends J, Christoffersen J. The nature of early caries lesions in enamel. Journal of Dental Research. 1986;65:2–11. [PubMed: 3510230]

[34]. Akkus A, Akkus A, Roperto R, Akkus O, Porto T, Teich S, et al. Evaluation of mineral content in healthy permanent human enamel by Raman spectroscopy. J Clin Exp Dent. 2016;8:e546–e9. [PubMed: 27957268]

[35]. Busch S Regeneration of human enamel. Angewandte Chemie. 2004;116:1452–5.

[36]. Hannig M, Hannig C. Nanomaterials in preventive dentistry. Nature nanotechnology. 2010;5:565–9.

[37]. Cao Y, Mei ML, Li Q-L, Lo ECM, Chu CH. Enamel prism-like tissue regeneration using enamel matrix derivative. Journal of dentistry. 2014;42:1535–42. [PubMed: 25193522]

[38]. Ning TY, Xu XH, Zhu LF, Zhu XP, Chu CH, Liu LK, et al. Biomimetic mineralization of dentin induced by agarose gel loaded with calcium phosphate. Journal of Biomedical Materials Research Part B: Applied Biomaterials. 2012;100:138–44. [PubMed: 21954134]

[39]. Lippert F, Parker DM, Jandt KD. In vitro demineralization/remineralization cycles at human tooth enamel surfaces investigated by AFM and nanoindentation. Journal of Colloid and Interface Science. 2004;280:442–8. [PubMed: 15533417]

[40]. Chen H, Tang Z, Liu J, Sun K, Chang S, Peters M, et al. Acellular synthesis of a human enamel-like microstructure. Adv Mater. 2006;14:1846.

[41]. Gandolfi M, P T, Siboni F, Modena E, De Stefano E, Prati C. Biomimetic remineralization of human dentin using promising innovative calcium-silicate hybrid “smart” materials. Dental Materials 2011;27:1055–69. [PubMed: 21840044]

[42]. Busch S, Schwarz U, Kniep R. Chemical and structural investigations of biomimetically grown fluorapatite-gelatin composit aggregates. Adv Funct Mater. 2003;13:189–98.

[43]. Chen H, Sun K, Tang Z, Law R, Mansfield J, Czajka-Jakubowska A, et al. Synthesis of fluoroapatite nanorods and nanowires by direct precipitation from solution. Cryst Growth Des. 2006;6:1504–8.

[44]. Cao C, Mei ML, Li L, Lo ECM, Chu CH. Methods of biomimetic remineralization of human dentine: a systematic review. Int J Mol Sci. 2015;16:4615–27. [PubMed: 25739078]

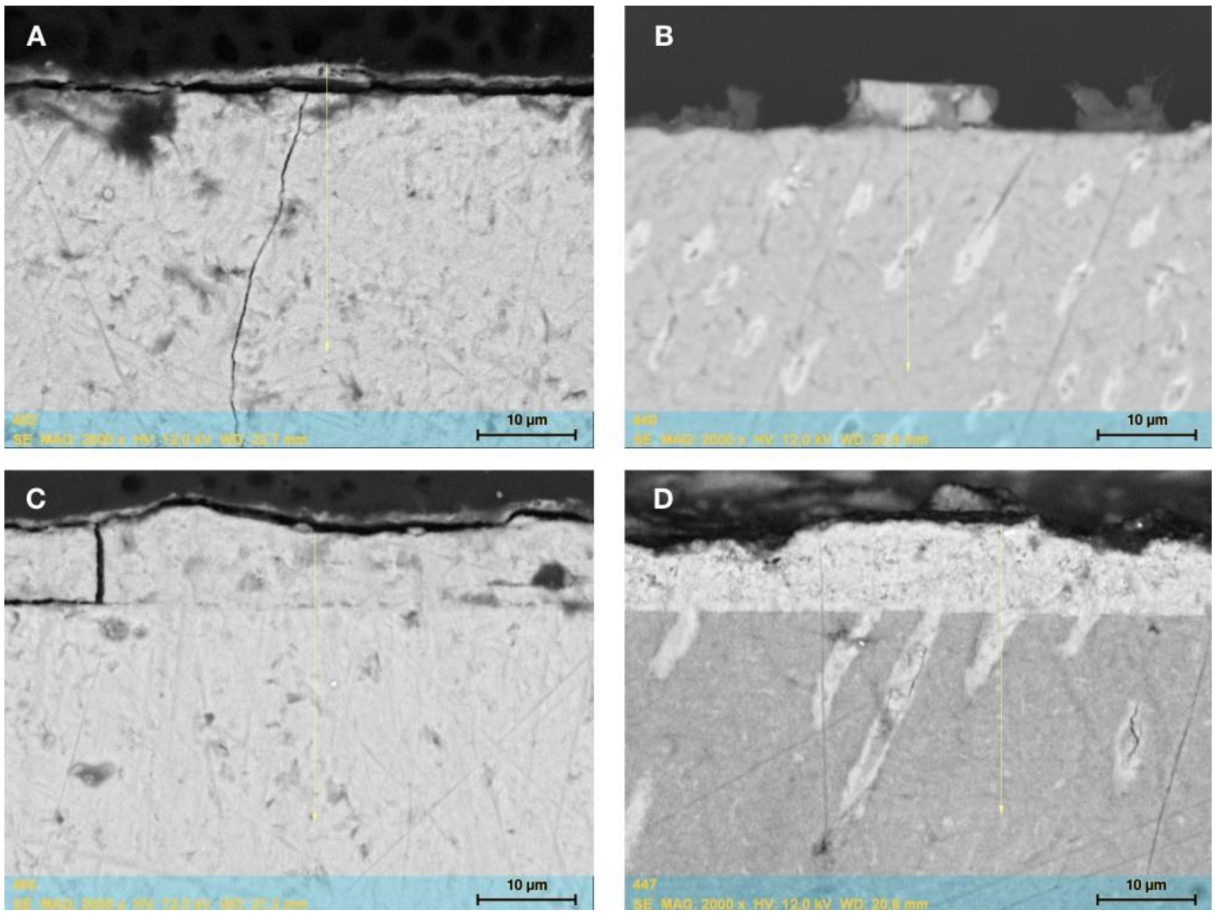

Figure 1:

SEM of representative enamel (A, C) and dentin samples (B, D). The enamel-like layer is visible on the surface of the treated samples. In dentin, the new mineral is also detectable in the tubules. Figures show the results after one (A, B) and five repeated applications (C, D) of BIMIN.

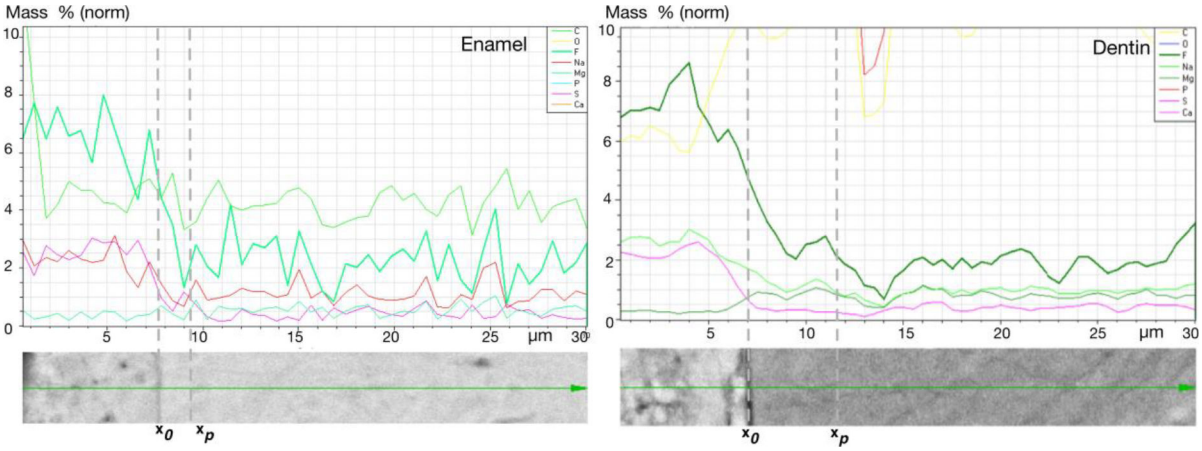

Figure 2:

SEM/EDX output of representative enamel and dentin samples after a 5-fold BIMIN application. Mass % of several elements (only results of fluoride, phosphate, and calcium are presented in the text) per measurement line (30 µm). From left to right: the first dotted line (x_0) separates the BIMIN layer from the sample surface and the second dotted line (x_p) limits the penetration zone in the tooth structure.

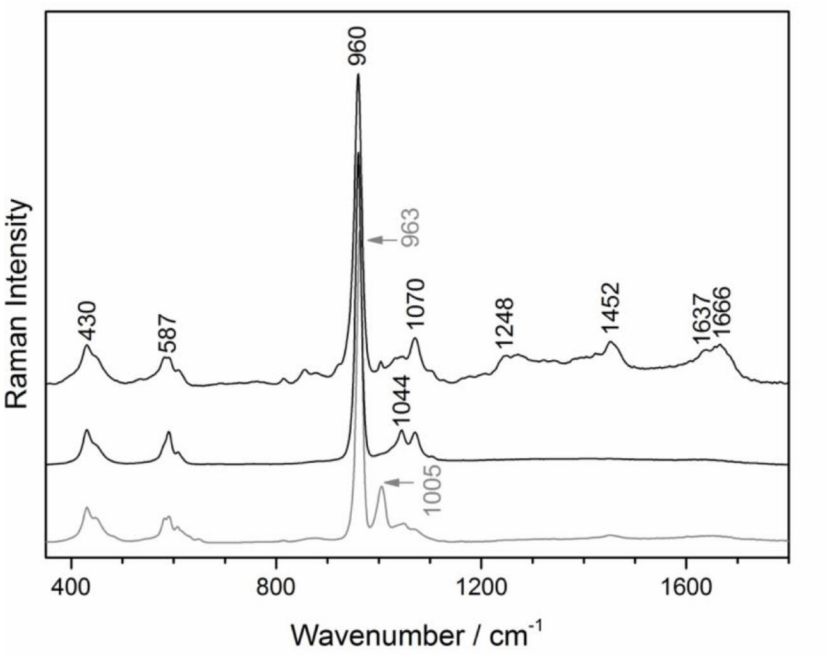

Figure 3:

Raman spectra from 350 to 1800 cm^{-1} of dentin (top), enamel (middle) and BIMIN (bottom). Labeled bands are discussed in the text. Spectra are shifted to avoid overlap.

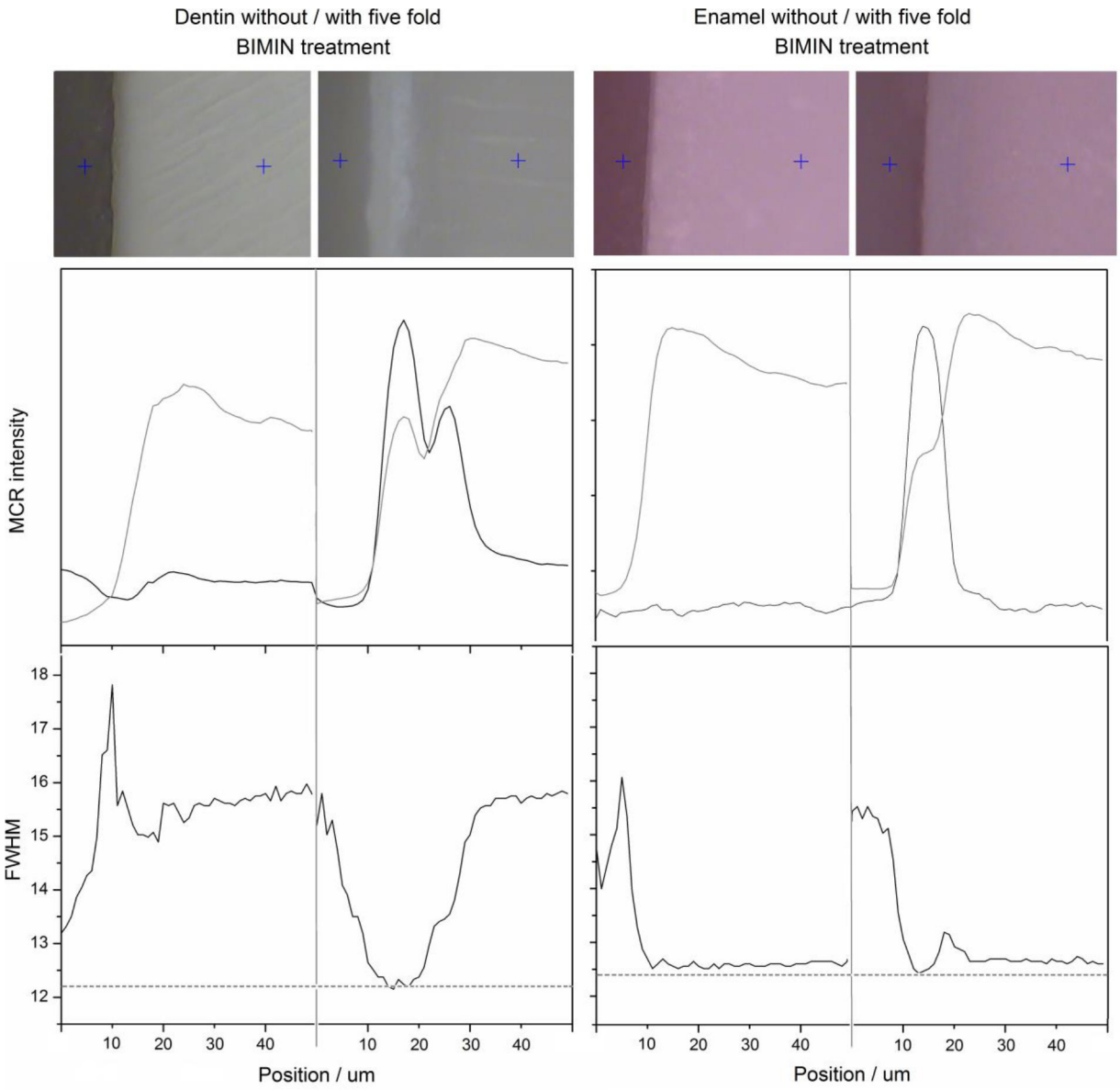

Figure 4:

Photomicrographs of dentin and enamel without and with BIMIN treatment (top row). Intensity of hydroxyapatite (gray trace) and BIMIN (black trace) components after multivariate curve resolution (MCR) analysis (middle row). Full width at half maximum of hydroxyapatite band near 960 cm^{-1} [30]. The distributions are plotted as a function of the lines from 0 to 50 μm.

Table 1:

Mineral content (mass concentration) of fluoride, phosphate, and calcium in treated (test; at BIMIN/hard tissue junction x_0) and untreated (control; at surface of hard tissue) samples measured using SEM/EDX.

	Mass concentration [%]			
	Enamel		Dentin	
	Test	Control	Test	Control
Fluoride	2.2 ± 0.9	1.6 ± 1.0	6.2 ± 2.1*	3.1 ± 1.2
Phosphate	15.6 ± 0.4	15.3 ± 0.7	13.7 ± 0.3	13.5 ± 0.6
Calcium	39.9 ± 3.4	38.2 ± 1.4	33.0 ± 1.7	32.4 ± 0.6

* $p < 0.001$ statistically significant different between test and controls